Qualitative Regulation of B Cell Antigen Receptor Signaling by CD19: Selective Requirement for PI3-Kinase Activation, Inositol-1,4,5-Trisphosphate Production and Ca^{2+} Mobilization

By Anne Mette Buhl,* Christopher M. Pleiman,§ Robert C. Rickert,‖ and John C. Cambier*‡

*From the *Division of Basic Sciences, Department of Pediatrics, National Jewish Medical and Research Center, 1400 Jackson Street, Denver, Colorado 80206; ‡Department of Immunology, University of Colorado Health Sciences Center, Denver, Colorado 80206; §Cadus Pharmaceuticals, 1601 Pierce St., Suite 110, Lakewood, Colorado 80214; and ‖Department of Biology, University of California San Diego, 9500 Gilman Drive, La Jolla, California 92093-0322*

Summary

Genetic ablation of the B cell surface glycoprotein CD19 severely impairs the humoral immune response. This requirement is thought to reflect a critical role of CD19 in signal transduction that occurs upon antigen C3dg coligation of antigen receptors with CD19 containing type 2 complement receptors (CR2). Here we show that CD19 plays a key accessory role in B cell antigen receptor signaling independent of CR2 coligation and define molecular circuitry by which this function is mediated. While CD19 is not required for antigen-mediated activation of receptor proximal tyrosines kinases, it is critical for activation of phosphatidylinositol 3-kinase (PI3-kinase). PI3-Kinase activation is dependent on phosphorylation of CD19 Y484 and Y515. Antigen-induced CD19-dependent PI3-kinase activation is required for normal phosphoinositide hydrolysis and Ca^{2+} mobilization responses. Thus, CD19 functions as a B cell antigen receptor accessory molecule that modifies antigen receptor signaling in a qualitative manner.

CD19 is a B-lymphocyte–specific transmembrane glycoprotein that is expressed from the pro–B cell until the plasma cell stage. CD19 appears to function in multiple capacities. It is a component of the type 2 complement receptor (CR2)[1] complex that contains CD19, CD21 (CR2), CD81, (TAPA-1), and Leu-13. CR2 is expressed by mature B cells and is activated upon binding of C3dg (reviewed in reference 1). Evidence indicates that CD19 may also be a constitutive component of the B cell antigen receptor (BCR) complex and is phosphorylated upon BCR crosslinking (2). Finally, although its ligand has not been identified, CD19 appears to function as a transducer in pro– and pre–B cells where it is expressed in the absence of CD21 and the BCR. The function of CD19 in these various contexts is poorly understood.

CD19 is a highly conserved protein containing two immunoglobulin-like domains in its extracellular aspect and nine potential tyrosine phosphorylation sites in its cytoplasmic tail (3). It is tyrosine phosphorylated upon cell activation in all three of the signaling contexts described above, presumably by Lyn, Fyn, or Lck associated with unligated CD19 (4–8). After phosphorylation, tyrosines Y^{484}XXM and Y^{515}XXM motifs have been shown to mediate the association of the p85-subunit of PI3-kinase with CD19 (9). In addition the proto-oncogene product Vav has been shown to associate with phosphorylated CD19 (10), presumably through the Y^{393}EEP motif which is predicted once phosphorylated to bind Vav (11). In vitro studies involving CD19 coimmunoprecipitated from stimulated Ramos B cells have demonstrated that tyrosine phosphorylated CD19 can interact with PI3-kinase, Fyn, PLCγ1 and GAP SH2 domains suggesting the interaction of multiple signaling molecules with the CD19 cytoplasmic tail (12, 13).

CD19 function has been studied primarily in the context of its role as a member of the CR2 receptor complex (14–16). CD19 signal transduction is activated by binding of the C3dg fragment of the C3 component of complement to CD21. Coligation of CD19 or CD21 with BCR causes a synergistic increase in a number of intracellular BCR-mediated signaling events, including Shc and Syk tyrosine phos-

[1] *Abbreviations used in this paper:* BCR, B cell antigen receptor; IP_3, inositol-1,4,5-trisphosphate; ITAM, immunoreceptor tyrosine based activation motif; NP, nitrophenol; PH, pleckstrin homology; PI, phosphatidylinositol; PI3-kinase, phosphatidylinositol 3-kinase.

 J. Exp. Med. © The Rockefeller University Press • 0022-1007/97/12/1897/14 $2.00
Volume 186, Number 11, December 1, 1997 1897–1910
http://www.jem.org

phorylation (17, 18), PLC-activation and calcium mobilization (19). Coligation also lowers the threshold for antigen stimulation of B cell proliferation (20) and enhances by ⩾10,000-fold the immunogenicity of antigen–complement complexes (HEL-C3dg) (21).

Antibody crosslinking of CD19 on certain immature B cell lines that do not express mIg has been shown to induce activation of Src-family kinases and tyrosine phosphorylation of CD19 and Vav (5, 13, 22). In this context CD19 crosslinking also results in PLC-activation, calcium mobilization and activation of the MAP kinase cascade (10, 19, 23).

Finally, anti-Ig stimulation of the BCR without CD19 cocrosslinking results in tyrosine phosphorylation of CD19, indicating that CD19 is a target of BCR-activated kinases (4, 5, 13). Also, anti-IgM stimulation of Daudi B cells leads to an increase in CD19 association with PI3-kinase (9). Consistent with this finding, several studies indicate that CD19 may be physically associated with the BCR. Incubation of B cells with Ig-specific mAb leads to mIg and CD19 comodulation and cocapping (24, 25). In Daudi B cells CD19 can be coimmunoprecipitated with mIgM (2). Whether CD21, Leu-13 and CD81 are required for the constitutive association of CD19 with the BCR is unknown; however CD19 expression levels in mature B cells appear to be about fivefold higher than CD21 expression levels (14) suggesting that CD19 occurs in both CD21-associated and -nonassociated forms.

Recent production of CD19 knockout mice have provided an opportunity to analyze B cell function in the absence of CD19 (26, 27). B cell development appears normal in these mice, but humoral immune responses are defective and B cells are unresponsive to antigen receptor stimulation as indicated by proliferation.

In this study we have investigated the constitutive role of CD19 in BCR-mediated signal transduction using CD19-deficient and -sufficient J558Lμm3CD45$^+$ plasmacytoma variants and primary B lymphocytes from CD19$^{-/-}$ and CD19$^{+/+}$ mice. Our results demonstrate a critical role for CD19 in antigen-mediated BCR activation of multiple signaling events. CD19 expression is required for detectable BCR-mediated PI3-kinase activation and for maximal phosphoinositide hydrolysis and calcium mobilization. The latter effects appear causally linked to failed PI3-kinase activation. Other more subtle effects of CD19 on BCR signaling include increased antigen-mediated Lyn and Syk tyrosine phosphorylation, but these are not attributable to enhanced PI3-kinase activation.

Materials and Methods

Reagents and Antibodies. The murine B cell plasmacytoma J558Lμm3 was provided by M. Reth (Max-Planck Institute for Immunology, Freiburg, Germany). We transfected this cell line previously to obtain a mouse full-length (B220) CD45$^+$-expressing variant (28). The human CD19 cDNA employed was provided by T. Tedder (Duke University Medical Center, Durham, NC). Rabbit polyclonal antibodies against CD19, Ig α, Syk, and Lyn, were prepared using GST fusion proteins produced in bacteria, purified by glutathione–Sepharose chromatography and cleaved with Factor Xa. Immunogens included the complete cytoplasmic tail for Igα, residues 1-131 for Lyn, the linker region for Syk (29), the SH3 domain for p85, and residues 411-547 of the CD19 cytoplasmic tail. The polyclonal antibody to the p85 subunit of PI3-kinase and mixed mouse monoclonals to PLCγ1 were purchased from UBI (Lake Placid, NY), anti-phosphotyrosine (AB-2) from Oncogene Science (Uniondale, NY), monoclonal anti-human CD19 from DAKO (Carpinteria, CA), and rabbit polyclonal to PLCγ2 from Santa Cruz Biochemicals (Santa Cruz, CA). Rabbit F(ab′)$_2$ antibody fragments to mouse IgG (H+L) (F(ab′)$_2$RAMIG) was purchased from Zymed Labs. (South San Francisco, CA). HRP-conjugated protein A (Zymed) and rat anti–mouse IgG1 (Zymed) were used for detection using the ECL detecting system (Amersham Corp., Arlington Heights, IL). R-phycoerythrin conjugate (PE-streptavidin) was from Biosource (Camarillo, CA). Indo-1 AM was from Molecular Probes Inc. (Eugene, OR). The inositol-1,4,5-trisphosphate [^{3}H] radioreceptor assay kit and *Myo*-[2-^{3}H(N)]-inositol (21.0 Ci/mmol) was purchased from DuPont-NEN (Boston, MA). Geneticin G418 was from GIBCO BRL (Gaithersburg, MD). Wortmannin was from Sigma Chem. Co. (St. Louis, MO). Nitrophenol (NP)$_9$BSA was prepared by coupling of BSA (10 mg/ml) in 3% $NaHCO_3$ to NP-CAP-OSu (Cambridge Research Biochemicals, Cambridge, UK) (40 mg/ml) in *N*,*N*-dimethyl formamide (DMF). After dialysis in $NaHCO_3$ and PBS the molecular ratio of NP to BSA was determined by measurement of the absorbance at OD_{430} with an extinction coefficient of 4230, pH 8.5 (NP molarity) and by Bradford analysis (BSA molarity). CD19$^{-/-}$ mice (27) were provided by R.C. Rickert and K. Rajewsky (University of Cologne, Cologne, Germany).

Cell Culture and Infection. The human CD19 cDNA was isolated from pMT2 by EcoR1 digest and subcloned into pSK Bluescript (Stratagene Inc., La Jolla, CA). The CD19 cDNA was then removed from pSK with HindIII/ClaI restriction digest and cloned into pLNCX (Williams, Fred Hutchinsen Cancer Center, Seattle, WA). This construct was electroporated into GP+E/NIH3T3 cells and cell supernatant collected at 72 h. To increase the virus titer, GP+E/NIH3T3 cells were incubated for 12 h in tunicamycin (1 μg/ml), and reinfected with pLNCX/hCD19 retrovirus by incubating with the cell supernatant collected above. After G418 selection (1 mg/ml), virus expressing clones were selected. Virus collected from these cells was then used to infect J558LμmCD45$^+$ myeloma cells. Polyclonal human CD19 positive J558Lμm 3CD45$^+$ cells were obtained after G418 selection by cell sorting of the bulk-infected population with a mouse monoclonal to human CD19. The cells were propagated in IMDM supplemented with 5% heat inactivated FCS (Hyclone Labs. Inc., Logan, UT), 50 U/ml penicillin and 50 μg/ml streptomycin and 1 mg/ml G418 (J558Lμm3CD45$^+$CD19$^+$) at 37°C with 7% CO_2. Mutation of CD19 tyrosines 484 and 515 to phenylalanines was performed by PCR using the primers TCCCAGTCCTTTGAGGATATG/CATATCCTCAAAGGACTGGGA for Y^{484} and GCAGACTCTTTTGAGAACATG/CATGTTCTCAAAAGAGTCTGC for Y^{515}. Mutated CD19 was inserted into pLNCX, packaged and used for infection as described above.

Analysis of Protein Tyrosine Phosphorylation. For stimulation cells were harvested, washed once in IMDM and resuspended at 10^7 cells/ml in IMDM. After 5 min incubation at 37°C, cells were stimulated with NP_9BSA (2.5 μg/ml), pelleted in a picofuge, resuspended in lysis buffer (10 mM Tris, pH 7.5, 150 mM NaCl, 1 mM EDTA, 1 mM Na_3VO_4, 10 mM NaF, 1% NP-40, 1 mM PMSF, and 2 μg/ml each of leupeptin, aprotinin, and α-1 antitrypsin), and then incubated on ice for 10 min. Lysates were cen-

trifuged for 5 min at 14,000 rpm. Cleared lysates were incubated with antibodies to signaling molecules and protein A–Sepharose or protein G–Sepharose at 4°C, washed four times in lysis buffer, boiled with reducing SDS sample buffer, and then fractionated on 10% SDS-PAGE. SDS-PAGE–fractionated proteins were subjected to electrophoretic transfer to PVDF membranes. Transfers were probed with antibodies and developed using the ECL detection system. Sequential immunoblotting for phosphotyrosine and effector was performed. For this purpose PVDF membranes were stripped in stripping buffer (100 mM 2-mercaptoethanol, 2% SDS, 62.5 mM Tris-HCl, pH 6.7) for 30 min at 54°C, washed and blocked before immunoblotting.

Flow Cytometric Analysis of $[Ca^{2+}]_i$ Mobilization. Cells were loaded with indo-1 AM and the intracellular $[Ca^{2+}]_i$ was monitored by flow cytometry (model 50H; Ortho Diagnostic Systems, Westwood, MA) as previously described (28). The mean $[Ca^{2+}]_i$ and percent of cells responding was determined with an appended data acquisition system and the MultiTIME software (Phoenix Flow Systems, San Diego, CA).

Measurement of Inositol Phosphate Generation. Inositol-1,4,5-trisphosphate generation was measured using a [^{3}H] radioreceptor assay kit (DuPont-NEN) according to the manufacturer's instructions. Generation of total inositol phosphates was measured as follows: cells were labeled for 18 h in 2 μCi/ml of *myo*-[2-^{3}H(N)]-inositol in inositol-free medium containing dialyzed 5% FCS before being washed in inositol-free media and incubated with inositol-free media containing 20 mM LiCl for 5 min. Cells were then stimulated for 25 min, lysed in 2 ml of methanol/HCl (99:1), and then 2 ml of chloroform was added. The aqueous phase was extracted, applied to a formate anion-exchange column, and then inositol phosphates were eluted with elution buffer (0.1 M formic acid, 1.0 M ammonium formate). Total [^{3}H] inositol incorporation was determined by measuring the radioactivity in the organic phase.

Assay for PI3-Kinase Activity. Cells were stimulated, lysed, and then immunoprecipitated for 1 h at 4°C using anti-p85 antibodies and protein A–Sepharose. PI3-kinase activity was measured as previously described (30). Samples were dried and reaction products resolved by thin-layer chromatography on precoated TLC Silica Gel 60 plates in $CHCl_3$/MeOH/2.5 M NH_4OH (9:7:2). The incorporation of $^{32}PO_4$ into phosphatidylinositol 3-phosphate was determined using a PhosphorImager.

Isolation of Splenic B Cells. Splenic B cells were prepared as previously described (31). In brief, spleens were excised from mice and cells were dispersed through a 100-μm mesh in IMDM. Red blood cells were lysed using Gey's solution. Total nucleated spleen preparations were depleted of T lymphocytes by complement-mediated lysis using HO13.4 and T24 antibodies and dense cells ($\rho \geqslant 1.066$) isolated by discontinuous Percoll density gradient centrifugation.

Results

Although tyrosine phosphorylation of CD19 after BCR ligation is well documented, the contribution of CD19 to BCR signaling is not defined. To study the role of CD19 in antigen-induced signal transduction we generated a wild-type CD19-positive and $Y^{484/Y515}$ to F CD19-positive variant of the J558Lμm3CD45$^+$ plasmacytoma. The parent clone expresses a NP-specific BCR and CD45, but does not express CD19 (28, 32). Human CD19 (hCD19) was introduced into this clone by retroviral infection, and lines (polyclonal populations) were isolated by G418 selection and fluorescence activated cell sorting of cells. Flow cytometric analysis revealed similar expression levels of sIgM,

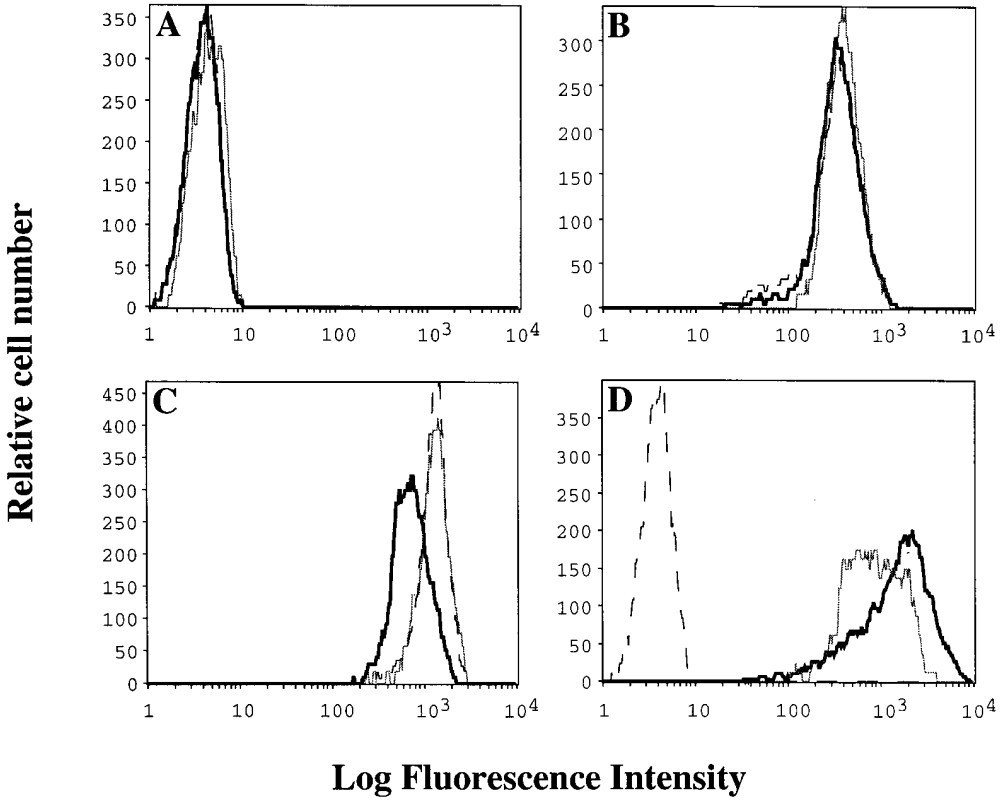

Figure 1. Expression levels of surface markers on the plasmacytoma cell lines. Flow cytometric analysis was performed on the J558Lμm3CD45$^+$ (*dotted lines*), J558Lμm3CD45$^+$CD19$^+$ (*thick lines*), and J558L μm3CD45$^+$ CD19$^+$ ($Y^{484}F,Y^{515}F$) (*thin lines*) cell lines. Shown is staining with secondary alone (*A*), biotinylated b-7-6 anti-IgM (*B*), biotinylated I32.5 anti-CD45 (*C*), or biotinylated HD37 anti-hCD19 (*D*) followed by PE-conjugated streptavidin.

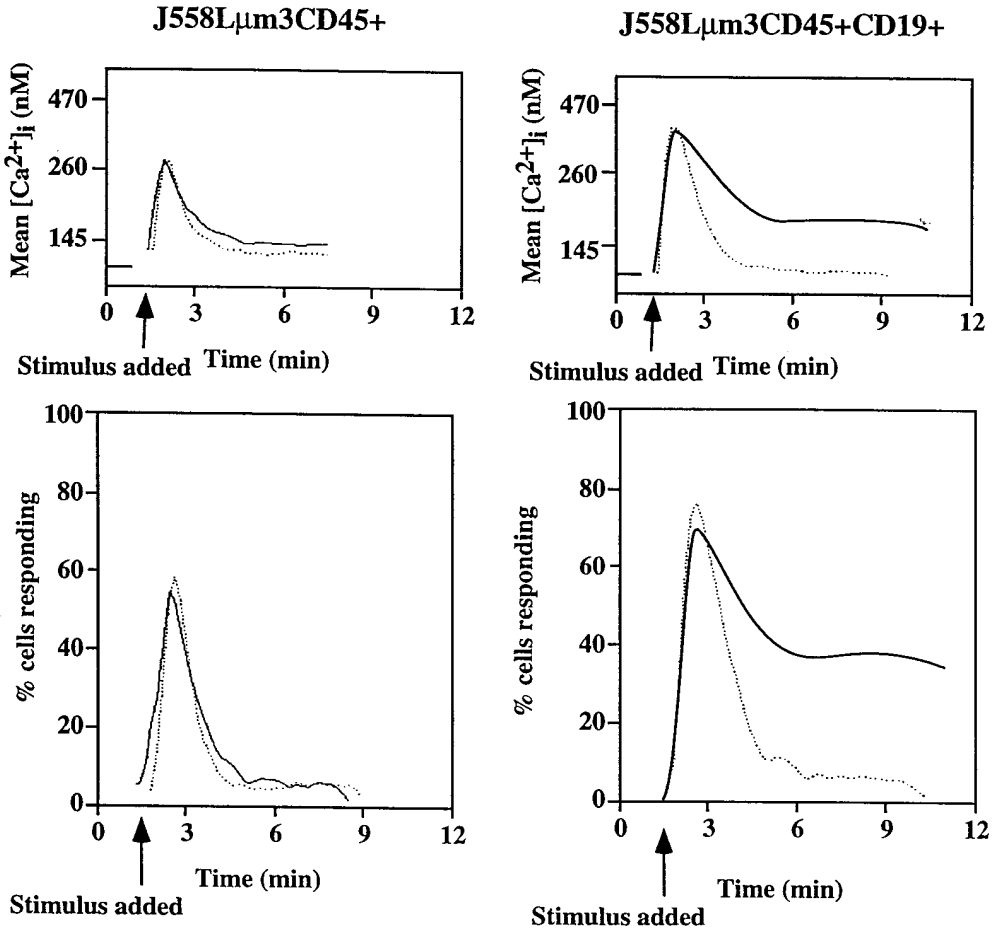

Figure 2. The CD19-negative and -positive J558Lμm3CD45$^+$ plasmacytoma variants mobilize $[Ca^{2+}]_i$ to different extent after antigen stimulation. J558Lμm3-CD45$^+$CD19$^-$ and J558Lμm3-CD45$^+$CD19$^+$ cells were loaded with indo-1 AM, and analysis of $[Ca^{2+}]_i$ initiated before antigen stimulation (250 ng NP_9BSA/10^6cells/ml). Mean $[Ca^{2+}]_i$ (*top*) and cells responding (*bottom*) after antigen stimulation of J558Lμm3-CD45$^+$CD19$^-$ and J558Lμm3-CD45$^+$CD19$^+$. The analysis was conducted under conditions of 60 nM (*dotted line*) or 1.3 mM (*solid line*) extracellular free calcium concentration buffered as calculated by the CalCalc program (74). $[Ca^{2+}]_i$ was calculated according to Grynkiewicz et al. (75). Approximately 600 cells were analyzed per second. $[Ca^{2+}]_i$ in resting cells is 100 nM.

CD45 and CD19 in the plasmacytoma cell lines (Fig. 1). Human CD19 was utilized since antibodies to mouse CD19 were not available at the time the studies were undertaken, and human and mouse CD19 are highly homologous (79% in nucleotide sequence, 75% in amino acid sequence) particularly in the cytoplasmic domain (3, 33). Recent studies indicate that human CD19 complements B cell function in CD19$^{-/-}$ mice (34). In addition, using a recently generated rat mAb, 1D3, specific for murine CD19 (35), Krop et al. (22) have demonstrated that murine CD19 shares with human CD19 an association with complement receptor CD21 and CD81, tyrosine phosphorylation, binding of PI3-kinase, and synergistic signaling with membrane IgM.

Antigen-stimulated Intracellular Ca^{2+} Release and Extracellular Ca^{2+} Influx Is Increased in Cells Expressing CD19. To investigate the differences in BCR signaling in the CD19-negative and -positive contexts, we loaded the J558Lμm3 CD45$^+$CD19-negative and CD19-positive variants with indo-1 AM and analyzed changes in intracellular free calcium concentration ($[Ca^{2+}]_i$) in response to antigen stimulation. Initially, this was done under conditions where the free calcium concentration in the medium ($[Ca^{2+}]_o$) was maintained at physiological levels of 1.3 mM. As shown in Fig. 2 (*solid lines*), antigen stimulation induced a rise in $[Ca^{2+}]_i$ in both cell lines; in the CD19-positive cell line the maximal mean $[Ca^{2+}]_i$ reached 430 nM while it was 260 nM in the CD19-negative cells. In the CD19-positive cell line, antigen stimulation also induced a much more prolonged increase in $[Ca^{2+}]_i$ than in the CD19-negative clone. To determine whether intracellular or extracellular calcium was responsible for the respective $[Ca^{2+}]_i$ increases, we added 3 mM EGTA at the time of initiation of analysis of $[Ca^{2+}]_i$. This results in buffering of $[Ca^{2+}]_o$ to a concentration of 65 nM (which corresponds to the $[Ca^{2+}]_i$ in resting cells) and prevents influx of extracellular calcium into the cell. Comparison of antigen-induced responses of CD19-negative and CD19-positive cells in low $[Ca^{2+}]_o$ (Fig. 2, *dotted lines*) indicated that optimal receptor-mediated release of calcium from intracellular stores requires CD19. Comparison of responses in high $[Ca^{2+}]_o$ revealed that influx is also dependent on the expression of CD19 (Fig. 2, *solid lines*).

Antigen Stimulation of Inositol-1,4,5-trisphosphate (IP_3) Production Is Dependent on CD19 Expression. To study CD19 dependence of signaling events upstream from calcium mobilization, we first compared antigen stimulation of IP_3 production in CD19-positive and -negative cells. IP_3 binds to its receptors on the ER leading to release of Ca^{2+} into the cytoplasm. Emptying of the ER stores triggers entry of calcium from the extracellular space by a mechanism known as capacitative Ca^{2+} entry (36). Thus, CD19 depen-

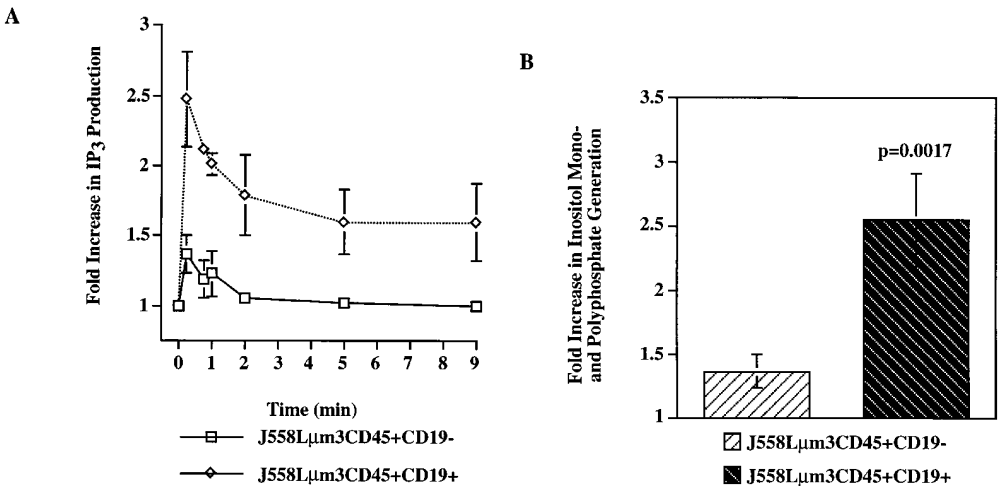

Figure 3. Antigen-induced IP_3 and total inositol phosphate release is greater in the CD19-positive than in CD19-negative J558Lμm3CD45$^+$ cells. (*A*) Cells (10×10^6/ml) were stimulated with 2.5 μg NP_9BSA for various times and the responses terminated by addition of 100% TCA (20% TCA final). After organic extraction the aqueous phase was assayed for IP_3 content in a [^{3}H]IP_3 receptor binding inhibition assay (NEN-DuPont). The results are expressed as fold increase of IP_3 release over basal (3 pmol $IP_3/2.5 \times 10^6$ cell equivalents). Shown is mean fold increase from three independent experiments ± standard error. (*B*) Cells were labeled with *Myo*-[2-^{3}H(N)]-inositol (21.0 Ci/mmol; 2 μCi/ml) in inositol-free medium containing 5% FCS at 10^6 cells/ml for 18 h and the generation of inositol phosphates was measured after stimulation of cells for 25 min with 2.5 μg $NP_9BSA/10^7$ cells/ml. The fold increase in inositol phosphate release was calculated; the two cell lines had comparable basal rates of inositol turnover as determined by the basal inositol phosphate release. Shown are the mean fold increases from three independent experiments ± standard error. Statistical significance was determined by JMP version 3.16 statistical software (SAS Institute, Cary, NC).

dence of IP_3 generation-induced response by antigen could explain the dependence of both intracellular calcium release and extracellular calcium influx on CD19 expression. Stimulation of the cell lines led to a very rapid and sustained rise in IP_3 production in the CD19-positive clone as measured using an IP_3-receptor binding inhibition assay (Fig. 3 *A*). Antigen stimulation of the CD19-negative clone led to rapid, but much more modest and only transient generation of IP_3. The kinetics and magnitude of IP_3 generation was consistent with those of calcium mobilization responses shown in Fig. 2 supporting the possibility that the attenuated calcium mobilization response may be caused by the attenuated BCR-mediated hydrolysis of PIP_2. We also measured the generation of [^{3}H]-inositol mono- and polyphosphates after antigen stimulation of *myo*-[2-^{3}H(N)]-inositol–labeled cell lines. As shown in Fig. 3 *B* the fold increase in total inositol mono- and polyphosphates generated during a 25-min stimulation was consistent with the mass measurement of IP_3 production (Fig. 3 *A*); stimulation of the CD19-positive clone led to an ~250% increase in inositol phosphate generation, while stimulation of the CD19-negative cell line induced an ~30% increase.

CD19 Expression Enhances BCR-mediated Protein Tyrosine Phosphorylation. Antigen stimulation is known to induce recruitment of Src- and Syk-family tyrosine kinases to Ig-α and Ig-β components of the BCR (37–39). The tyrosine kinases bind via their SH2-domains to immunoreceptor tyrosine based activation motif (ITAM) phosphotyrosines and this leads to secondary recruitment, phosphorylation, and activation of downstream signaling molecules such as PLCγ1, PLCγ2, and PI3-kinase (reviewed in reference 40). To define the effects of CD19 expression on these phosphorylation events we stimulated CD19-negative and -positive cell lines, immunoprecipitated intracellular signaling molecules and conducted anti-phosphotyrosine immunoblotting analysis. The spectra of phosphoproteins in whole cell lysates from the J558Lμm3CD45$^+$CD19$^-$ and the J558Lμm3CD45$^+$CD19$^+$ cell lines looked similar with the exception of the presence of a tyrosine phosphorylated CD19 in the CD19-positive cell lysate (results not shown). Induced phosphorylation of several signaling molecules was analyzed after stimulation with normalization of immunoprecipitation and lane loading by sequential antieffector immunoblotting. We studied tyrosine phosphorylation after 1 min of antigen stimulation since we have shown previously that effector enzymes under study are maximally phosphorylated at this time in the J558Lμm3CD45$^+$ plasmacytoma (41). As shown in Fig. 4, CD19 expression led to modest increases in antigen-induced tyrosine phosphorylation of Ig-α, Lyn, Syk, PLCγ1, and PLCγ2. Quantitation of tyrosine phosphorylation by scanning densitometry (at least three independent experiments for each effector enzyme) and normalization to effector levels revealed increased phosphorylation of Ig-α, Lyn, and Syk by 1.5–2-fold in the CD19-positive line. Induced PLCγ1 and PLCγ2 tyrosine phosphorylation was 2.5–3-fold higher in the CD19-positive cell line than in the CD19-negative cell line. These results suggest that CD19 functions in part by increasing the magnitude of certain proximal BCR coupled tyrosine phosphorylation events.

Antigen Stimulation of PI3-Kinase Activation Is Severely Impaired in the CD19-negative J558Lμm3CD45$^+$ Plasmacytoma. CD19 contains two cytoplasmic YXXM motifs that mediate its association with the p85 subunit of PI3-kinase after phosphorylation of the tyrosines (9). The phosphorylation of these tyrosines may contribute to BCR-mediated PI3-kinase activation. We determined the activity of PI3-kinase in the cell lines by measuring the PI3-kinase activity associated with anti-p85 immunoprecipitates after stimulation with NP_9BSA for 2 min. The results shown in Fig. 5 demonstrate a 250% increase in PI3-kinase activity in the CD19-positive cell line after antigen stimulation, but only a 40% increase in the CD19-negative variant. The residual

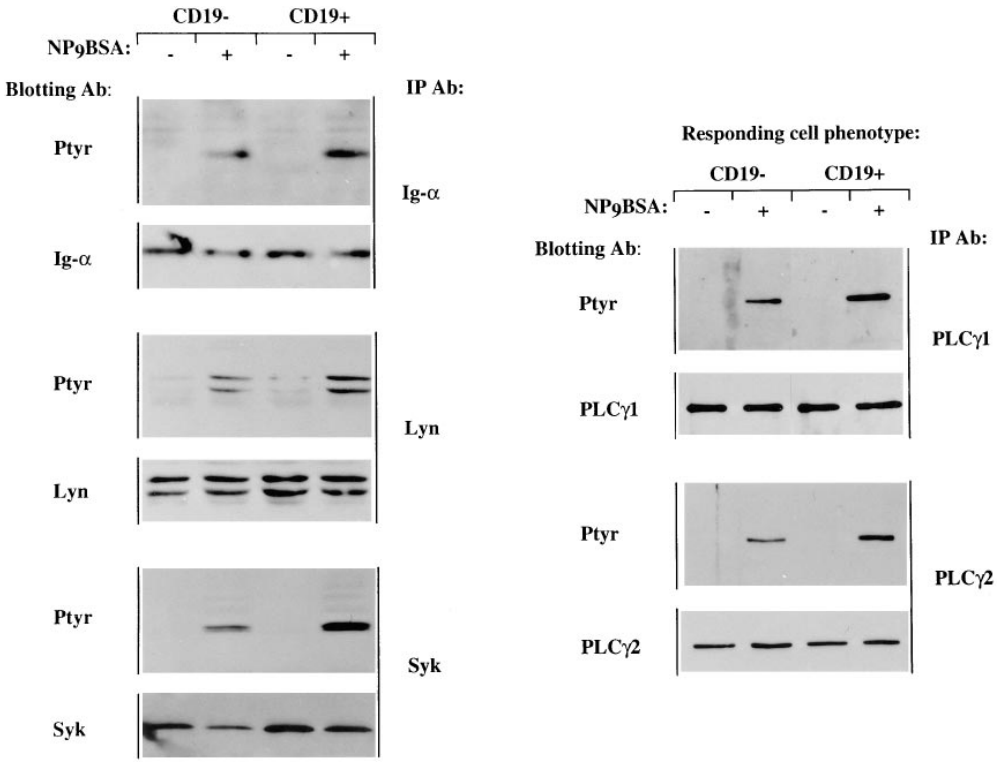

Figure 4. Tyrosine phosphorylation of signaling molecules upon antigen stimulation of the CD19-negative and CD19-positive cell lines. J558Lμm3 $CD45^+$ variants were stimulated for 1 min with 2.5 μg $NP_9BSA/10^7$cells/ml, lysed, and intermediary signaling molecules immunoprecipitated with various antibodies and fractionated on 10% SDS-PAGE. After electrophoretic transfer to PVDF membrane, both anti-phosphotyrosine and anti-effector immunoblotting were performed. Data are representative of at least three independent experiments.

activation of PI3-kinase in the absence of CD19 expression is probably a result of PI3-kinase activation through interaction with SH3 domains of Src-family kinases (42). The results described above are summarized in the two first columns of Table 1. It is clear that CD19 influences multiple intracellular signaling events. Some signaling events are only slightly increased in the CD19-positive cell line, (i.e., Ig-α, Lyn, and Syk tyrosine phosphorylation) while others are almost totally dependent on expression of CD19 (i.e., IP_3 generation, calcium influx, and PI3-kinase activation).

Wortmannin Inhibits Antigen-induced $[Ca^{2+}]_i$ Mobilization and IP_3 Generation in the J558Lμm3CD45$^+$CD19$^+$ Plasmacytoma. To begin to dissect the relationship among the observed CD19 effects, we assessed the effects of the PI3-kinase inhibitor wortmannin on signaling events. Wortmannin has been shown to inhibit PI3-kinase activity by covalent modification of a lysine residue in the PI3-kinase catalytic subunit, p110 (43). We also used the competitive PI3-kinase inhibitor Ly294002 (44) and obtained similar results as in our studies with wortmannin (results not shown). The effect of wortmannin on antigen-induced activation of PI3-kinase was determined. The results shown in Fig. 6 *A* demonstrate the inhibitory effect of wortmannin on antigen-mediated PI3-kinase activation in the J558Lμm3CD45$^+$ CD19$^+$ plasmacytoma. Cells were pretreated for 30 min with DMSO (vehicle) or increasing concentrations of wortmannin, stimulated with antigen for 2 min, washed, and then lysed before PI3-kinase was immunoprecipitated and activity measured in an in vitro kinase assay with phosphatidylinositol (PI) containing vesicles as substrate. Consistent with its previously established IC_{50}, 10 nM wortmannin inhibited the antigen-mediated PI3-kinase activation by 54%, and 25 nM wortmannin inhibited 75% of antigen-induced PI3-kinase activity. Wortmannin added to the cells immediately before washing and lysis did not effect the PI3-kinase activity

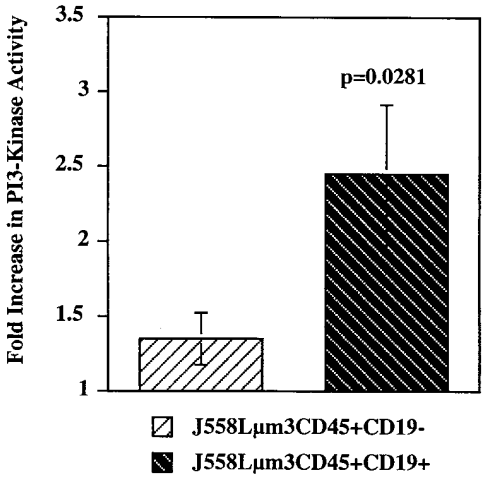

Figure 5. PI3-kinase activity is significantly increased only upon antigen stimulation of the CD19-positive J558Lμm3$CD45^+$ cells. CD19-negative and CD19-positive J558Lμm3$CD45^+$ cells were stimulated for 2 min with 1 μg$NP_9BSA/4 \times 10^6$/ml, lysed and PI3-kinase immunoprecipitated with anti-p85 antibody. Immunoprecipitates were washed and assayed for P-I3 kinase activity. Fold increase in PI3-kinase activity after stimulation was determined using a PhosphorImager. The data shown is the mean fold increase over basal in eight independent experiments ± standard error of the mean. Statistical significance was determined by JMP version 3.16 statistical software (SAS Institute, Cary, NC).

Table 1. *Phenotypic Differences Between J558Lμm3CD45$^+$CD19$^-$ and J558Lμm3CD45$^+$CD19$^+$ Cell Lines*

	Responding cell phenotype/condition		
Signal transduction event	CD19$^+$	CD19$^-$	CD19$^+$ with 25 nM wortmannin
Ig-αTyr Phos	++++	+++	++++
Lyn Tyr Phos	++++	+++	++++
Syk Tyr Phos	++++	+++	++++
PLCγl/PLCγ2 Tyr Phos	++++	++	+++
IP_3 production	++++	+	+
[Ca^{2+}]i mobilization			
Intracellular stores	++++	++	++
Influx	+++	−	−
PI3-Kinase activation	++++	+	+

(data not shown) indicating that the inhibitor was acting intracellularly.

To investigate the influence of PI3-kinase on the BCR-mediated calcium mobilization seen in the CD19-positive cell line, we preincubated the cells with increasing concentrations of wortmannin and measured the antigen-induced increase in $[Ca^{2+}]_i$. As shown in Fig. 6 *B*, wortmannin strongly inhibited Ca^{2+} mobilization in the J558Lμm3CD45$^+$ CD19$^+$ cells. Sensitivity to wortmannin was also evident in the IP_3 generation response. A wortmannin concentration of 25 nM strongly inhibited IP_3 production in the J558Lμm3 CD45$^+$CD19$^+$ cell line after 1 minute of antigen stimulation (Fig. 6 *C*). In both cases wortmannin at a concentration of 25 nM converted the phenotype of the CD19-positive cells essentially to that of the CD19-negative cells. This result was consistent with the 75% inhibition of PI3-kinase activation by 25 nM wortmannin in Fig. 6 *A* and indicates that the CD19 requirement for IP_3 production and calcium mobilization may be attributable to PI3-kinase activation. Interestingly, wortmannin inhibited the residual antigen-stimulated PI3-kinase activation, IP_3 production, and Ca^{2+} mobilization of the CD19-negative cell line (data not shown) consistent with the possible absolute dependence of these responses on PI3-kinase activation.

Induced Tyrosine Phosphorylation of Intracellular Effector Enzymes Is Insensitive to Wortmannin. To investigate the potential role of CD19-activated PI3-kinase on early BCR-mediated protein tyrosine phosphorylation events, CD19-positive cells were preincubated for 30 min with DMSO (vehicle) or increasing concentrations of wortmannin and stimulated for 1 min with antigen before effectors were immunoprecipitated and analyzed. As shown in Fig. 7, antigen-induced tyrosine phosphorylation of Ig-α, Lyn, and Syk was insensitive to wortmannin. PLCγ1 and PLCγ2 tyrosine phosphorylation was somewhat sensitive to wortmannin preincubation although the decrease in induced tyrosine phosphorylation was modest (35% inhibition at 25 nM wortmannin, Table 2) compared with the degree of wortmannin inhibition of IP_3 generation and calcium mobilization (91.5% inhibition, Table 2). It seems very unlikely that the >90% inhibition of PLCγ activity could be caused by a 35% inhibition of PLCγ phosphorylation Thus, as summarized in Table 1, CD19 expression by the J558Lμm3 CD45$^+$ plasmacytoma is required for optimal antigen stimulation of multiple intracellular signaling events, but only some of these are secondary to the nearly absolute dependence of PI3-kinase activation on CD19.

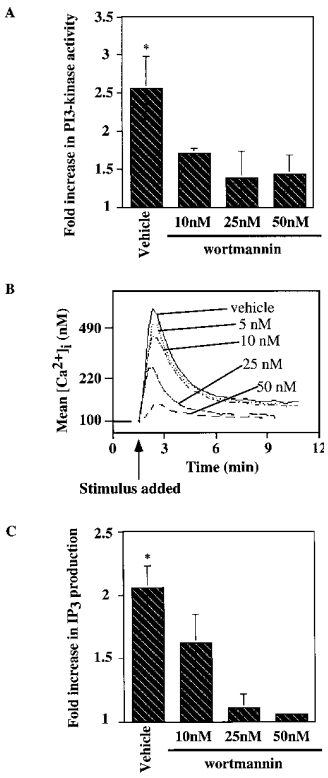

Figure 6. Wortmannin inhibits the antigen-induced increase in PI3-kinase activity, $[Ca^{2+}]_i$ mobilization and IP_3 generation in the J558Lμm3 CD45$^+$CD19$^+$ plasmacytoma. (*A*) Cells were preincubated with DMSO (vehicle) or wortmannin at various concentrations (in 0.2% final DMSO concentration) for 25 min at 25°C, prewarmed for 4 min at 37°C, and then stimulated for 2 min with 1 μg $NP_9BSA/4 \times 10^6$ cells/ml before analysis of PI3-kinase activation as described in Fig, 4. Shown is the mean fold increase in activity over basal from four independent experiments ± standard error of the mean. Asterisk indicates a statistical significance of $P < 0.05$ determined by JMP 3.16 statistical software. (*B*) To study the effects of wortmannin on the calcium response, J558Lμm3CD45$^+$CD19$^+$ cells were Indo-1 AM loaded and preincubated with DMSO (vehicle) or wortmannin at various concentrations (resulting in 0.2% final DMSO) for 25 min at 25°C, prewarmed for 4 min at 37°C, and stimulated at arrow with 250 ng $NP_9BSA/10^6$ cells/ml. Shown is the mean $[Ca^{2+}]_i$ over time with analysis of ~600 cells/s. $[Ca^{2+}]_i$ in resting cells is 100 nM. (*C*) J558Lμm3CD45$^+$CD19$^+$ cells were preincubated with DMSO or increasing concentrations of wortmannin, prewarmed, and stimulated with 2.5 μg $NP_9BSA/10^7$/ml for 1 min before IP_3 production was measured by the IP_3 receptor binding inhibition assay. Shown is the mean fold increase over basal in three independent experiments ± standard error of the mean. Asterisk indicates a statistical significance of $P < 0.05$ determined by JMP 3.16 statistical software.

Mutation of p85 Binding Sites Destroy the Ability of CD19 to Mediate an Increase in BCR-mediated $[Ca^{2+}]_i$ Mobilization. To further explore the requirement of CD19 for PI3-kinase activation and optimal antigen-mediated $[Ca^{2+}]_i$ mobilization, we introduced a double-point mutant of CD19, CD19Y^{484}F,Y^{515}F, into the J558Lμm3CD45$^+$ plasmacytoma. The expression levels of sIgM, CD45 and CD19 (Y^{484}F,Y^{515}F) in this cell line is shown in Fig. 1. It has previously been demonstrated that the mutations Y^{484}F and Y^{515}F abrogates the ability of CD19 to interact with the p85-subunit of PI3-kinase (9). Like the CD19-negative cell line, the CD19 mutant cell line, showed no significant anti-

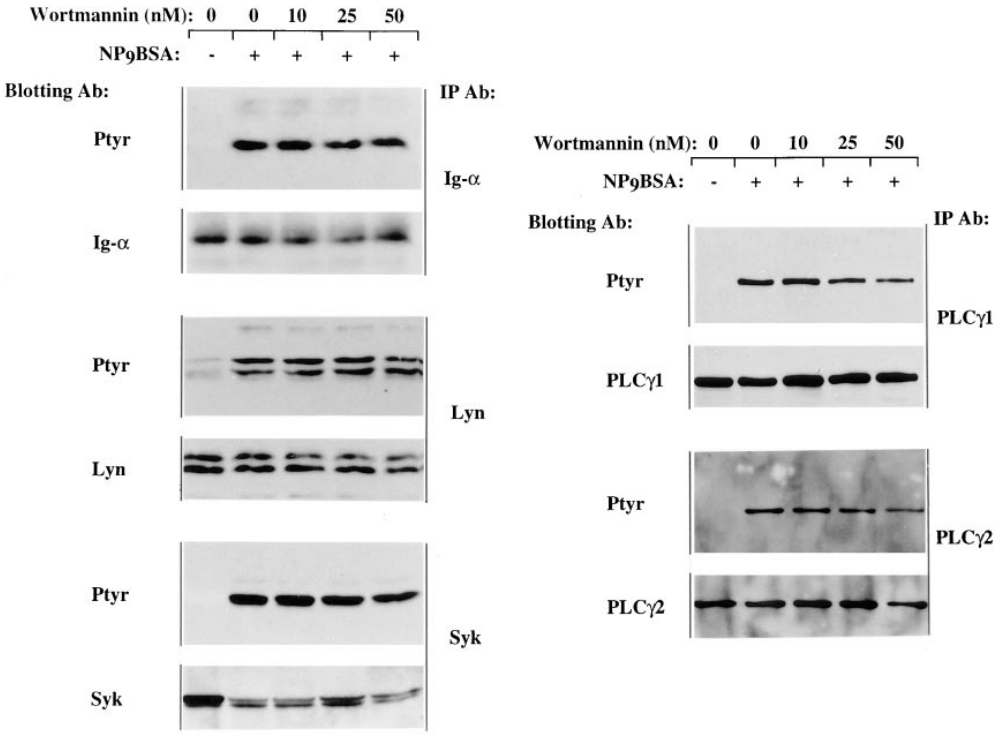

Figure 7. In the CD19-positive J558Lμm3CD45$^+$ cells, antigen-induced tyrosine phosphorylation of PLCγ1 and PLCγ2 is slightly inhibited by wortmannin, while Lyn, Ig-α and Syk inductive tyrosine phosphorylation is insensitive to wortmannin. J558Lμm3CD45$^+$CD19$^+$ cells were preincubated with DMSO or increasing concentrations of wortmannin, prewarmed and stimulated for 1 min with NP_9BSA (2.5 μg/10^7 cells/ml) and lysed. Immunoprecipitation, SDS-PAGE fractionation and electrophoretic transfer were performed. For each immunoprecipitation, both anti-phosphotyrosine and anti-effector immunoblots are shown. Results are representative of at least three independent experiments.

gen-mediated activation of PI3-kinase (results not shown). When we assayed the ability of the cell line expressing the mutant CD19 to mobilize $[Ca^{2+}]_i$ in response to antigen stimulation, we found that the mutant CD19 cell line behaved equivalently to the J558Lμm3CD45$^+$ cell line (Fig. 8). This suggests that both CD19-mediated increase in BCR-induced PI3-kinase activation and Ca^{2+} mobilization require phosphorylation of CD19 Y^{484} and Y^{515}.

Wortmannin Inhibits Antigen-stimulated $[Ca^{2+}]_i$ Mobilization in Splenic B Cells. To investigate the role of PI3-kinase in antigen-induced signaling in a more physiological system, we purified splenic B cells (ρ ⩾1.066) from spleens of normal mice and assessed the effects of wortmannin on BCR signaling. After preincubation for 30 min with DMSO or wortmannin, splenic B cells were stimulated with 13.2 μg/10^6 cells $F(ab')_2$RAMIG. As observed in the J558L μm3CD45$^+$CD19$^+$ cell line, wortmannin inhibited, as a function of its concentration, the antigen-mediated calcium mobilization in these primary B cells (Fig. 9). Wortmannin also inhibited the residual antibody-mediated Ca^{2+} mobilization in CD19$^{-/-}$ splenic B cells (data not shown). Thus, BCR signaling in J558Lμm3CD45$^+$CD19$^+$ and normal B cells is similarly sensitive to PI3-kinase inhibition and CD19 function (see below).

CD19 Is Required for Anti-BCR Stimulation of PI3-Kinase Activation and Ca^{2+} Mobilization in Splenic B Cells. To extend our observations regarding CD19 dependence of BCR-mediated signaling in B lymphocytes we compared BCR-mediated PI3-kinase activation and calcium mobilization responses of B cells from CD19 knockout mice and normal mice. It has previously been reported that no distinguishable difference can be seen between CD19-deficient and normal B cells in the pattern or the degree of substrate phosphorylation after surface immunoglobulin stimulation (27). We obtained the same results when comparing whole cell lysates from CD19$^{-/-}$ and CD19$^{+/+}$ cells (results not shown). However, careful investigation of several signaling events revealed that ρ ⩾1.066 resting splenic B lymphocytes from CD19$^{-/-}$ mice are impaired in their response to surface immunoglobulin crosslinking when compared with CD19$^{+/+}$ littermates. $F(ab')_2$RAMIG-mediated PI3-kinase activation was severely diminished in the CD19$^{-/-}$ B cells (Fig. 10), reminiscent of the situation in the plasmacytoma cell lines. As shown in Fig. 11, absence of CD19 also clearly affects

Table 2. *Percent Inhibtion of Maximal Responses by Wortmannin Preincubation*

	IP_3 production	PLCγ1 tyrosine phosphorylation	PLCγ2 tyrosine phosphorylation
10 nM	41.7 ± 10.8% (n = 2)	18.2 ± 5.6% (n = 2)	16.3 ± 4.4% (n = 6)
25 nM	91.5 ± 8.6% (n = 2)	34.6 ± 11.4% (n = 3)	34.9 ± 7.4% (n = 5)
50 nM	97.6 ± 2.5% (n = 2)	44.7 ± 10.2% (n = 3)	58.4 ± 3.8% (n = 6)

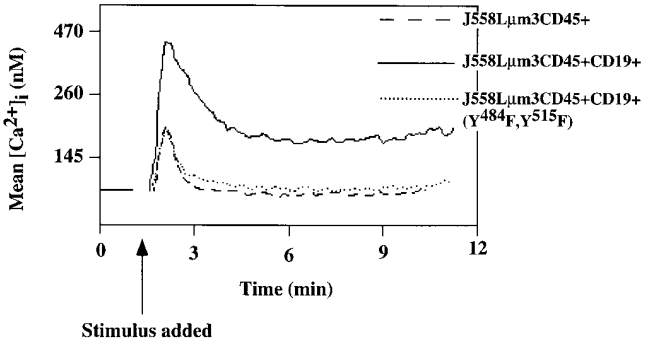

Figure 8. Mutant CD19 (CD19Y^{484}F,Y^{515}F) does not support antigen-induced $[Ca^{2+}]_i$ mobilization. J558Lμm3CD45$^+$CD19$^-$, J558Lμm3CD45$^+$ CD19$^+$ and J558Lμm3CD45$^+$CD19$^+$(Y^{484}F,Y^{515}F) cells were loaded with Indo-1 AM, and analysis of $[Ca^{2+}]_i$ initiated before antigen stimulation (250 ng $NP_9BSA/10^6$cells/ml). Shown is the mean $[Ca^{2+}]_i$ over time with analysis of ~600 cells/s. $[Ca^{2+}]_i$ in resting cells is 100 nM.

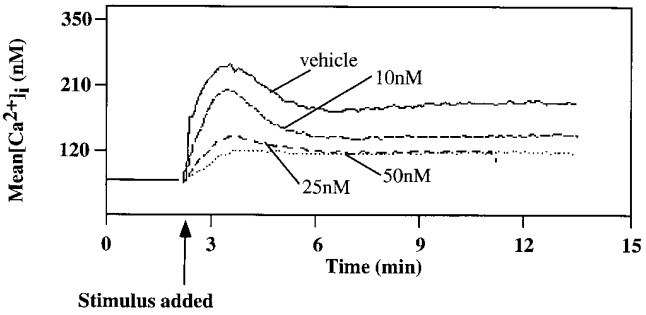

Figure 9. Antigen induction of $[Ca^{2+}]_i$ mobilization in splenic B cells from normal mice is sensitive to wortmannin. Splenic B cells (ρ ⩾1.066) were isolated from spleens of normal mice, and loaded with Indo-1 AM. The cells were preincubated with DMSO or increasing concentrations of wortmannin for 25 min at 25°C. They were then warmed to 37°C for 4 min and stimulated with 13.2 μg $F(ab')_2$RAMIG/10^6/ml (at arrow). Shown is the mean $[Ca^{2+}]_i$ over time with analysis of ~600 cells/s. $[Ca^{2+}]_i$ in resting cells is 70 nM.

BCR-mediated calcium mobilization. A decrease in calcium mobilization was seen in B lymphocytes from the CD19$^{-/-}$ mice in response to stimulation with an optimal dose of antibody (Fig. 11 *A*). At suboptimal concentrations of antibody (1.3 μg $F(ab')_2$RAMIG) almost no BCR-mediated calcium mobilization was seen in cells from CD19$^{-/-}$ mice, while cells from the CD19$^{+/+}$ littermates still responded well (Fig. 11 *B*). We obtained equivalent results in 10 independent experiments. Our results appear to conflict with those of Sato et al.(34), who observed enhancement of later phase Ca^{2+} mobilization in CD19$^{-/-}$ cells. These contrasting findings may result from technical differences in the respective studies.

Discussion

Recent studies of CD19$^{-/-}$ mice and CD19 transgenic mice have demonstrated the importance of CD19 in B cell development, but particularly in the immune response of mature B cells. In human CD19 transgenic mice B cell development is impaired (45) as indicated by the fact that these mice have dramatically fewer B cells in the periphery. In these transgenic animals proper B cell development is very sensitive to even small increases in CD19 expression levels (46). CD19$^{-/-}$ mice also have lower levels of B cells in the periphery, and mature B cells from these animals mount a poor proliferative response to anti-BCR antibodies. These animals respond only weakly to T cell–dependent antigens, germinal center formation is lacking or diminished, and the serum immunoglobulin levels are significantly reduced (26, 27, 47). Based on these findings, it has been suggested that CD19 functions by enhancing the cellular sensitivity to antigen, setting the threshold for antigen-mediated signaling (46). This may reflect a CR2-dependent coreceptor function and/or an accessory function of CD19 in BCR signal transduction.

Here we have defined an important accessory function for CD19 in antigen-induced BCR signal transduction and described a molecular basis for this accessory function. CD19 was found to influence the magnitude of activation

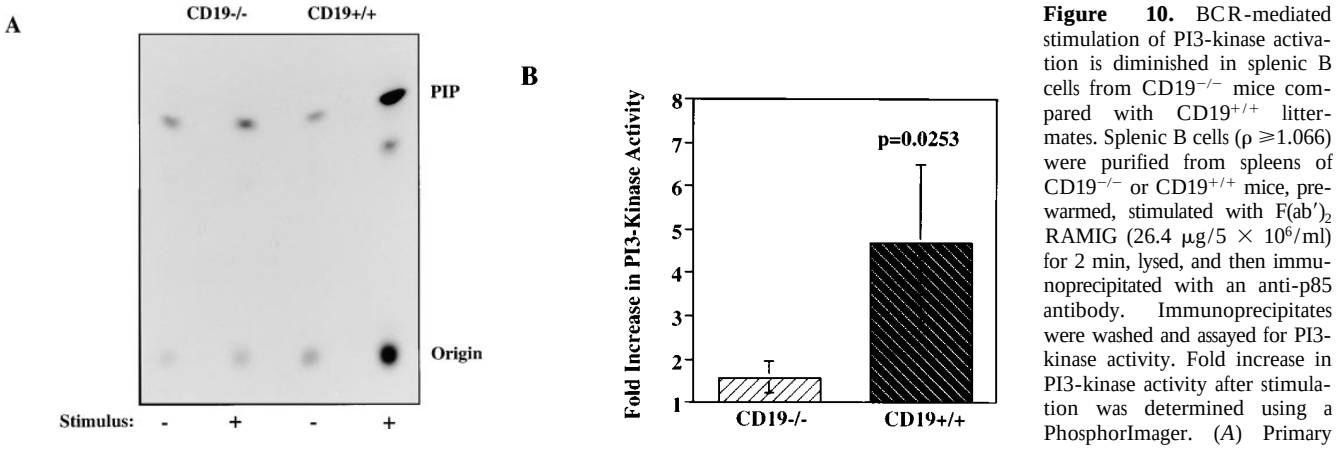

Figure 10. BCR-mediated stimulation of PI3-kinase activation is diminished in splenic B cells from CD19$^{-/-}$ mice compared with CD19$^{+/+}$ littermates. Splenic B cells (ρ ⩾1.066) were purified from spleens of CD19$^{-/-}$ or CD19$^{+/+}$ mice, prewarmed, stimulated with $F(ab')_2$ RAMIG (26.4 μg/5 × 10^6/ml) for 2 min, lysed, and then immunoprecipitated with an anti-p85 antibody. Immunoprecipitates were washed and assayed for PI3-kinase activity. Fold increase in PI3-kinase activity after stimulation was determined using a PhosphorImager. (*A*) Primary autoradiographic data from a representative experiment. (*B*) Mean fold increase over basal in three independent experiments ± standard error of the mean. Statistical significance was determined by JMP version 3.16 statistical software (SAS Institute).

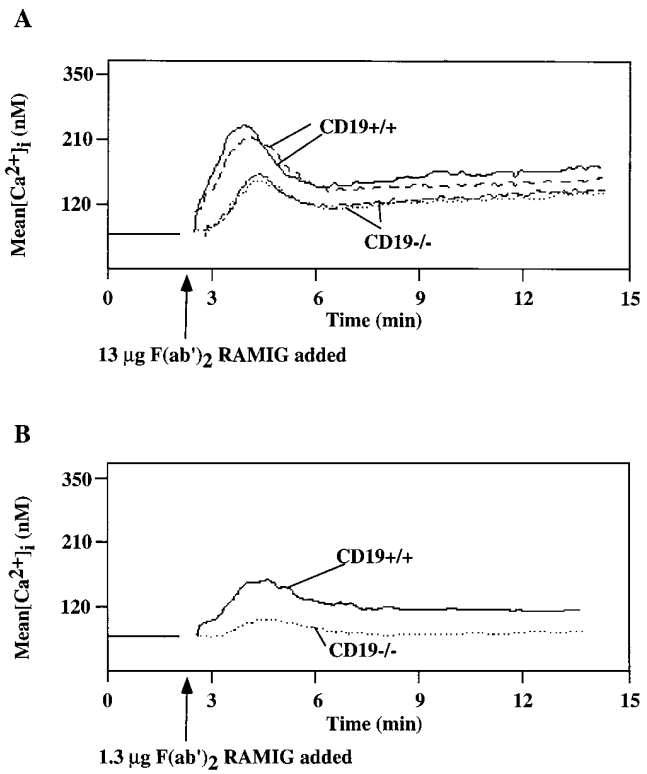

Figure 11. BCR-mediated $[Ca^{2+}]_i$ mobilization is reduced in splenic B cells from $CD19^{-/-}$ mice compared with $CD19^{+/+}$ littermates at both optimal and suboptimal doses of antibody. B cells ($\rho \geq 1.066$) were isolated from spleen of $CD19^{-/-}$ and $CD19^{+/+}$ mice and loaded with Indo-1 AM. $[Ca^{2+}]_i$ mobilization was monitored before and after stimulation of the cells with $F(ab')_2$ RAMIG. (*A*) Cells were stimulated with 13 $\mu g/10^6$ cells/ml; shown is an overlay of the $[Ca^{2+}]_i$ mobilization pattern in an experiment where splenic B cells from two $CD19^{-/-}$ and two $CD19^{+/+}$ mice were compared independently. This experiment was performed 10 times with similar results. (*B*) Cells were stimulated with a suboptimal dose of $F(ab')_2$ RAMIG (1.3 $\mu g/10^6$ cells/ml). Shown is the mean $[Ca^{2+}]_i$ over time with analysis of ~600 cells/s. $[Ca^{2+}]_i$ in resting cells is 70 nM.

of multiple intracellular signaling pathways after antigen stimulation of the BCR. While expression of CD19 leads to modestly enhanced antigen-induced Ig-α, Lyn, Syk, PLCγ1, and PLCγ2-inductive tyrosine phosphorylation, CD19 is absolutely required in order to obtain substantial PI3-kinase activation, IP_3 generation, and maximal calcium mobilization. Thus, CD19 modifies BCR signaling in a qualitative manner. Using the PI3-kinase inhibitor wortmannin we further determined that while the increased antigen-induced tyrosine phosphorylation of Ig-α, Lyn, and Syk is independent of PI3-kinase activation, differences in IP_3 turnover and calcium mobilization are a function of PI3-kinase activation. Results obtained in CD19-positive and -negative variants of the J558Lμm3$CD45^+$ plasmacytoma cells were confirmed using primary B lymphocytes from $CD19^{-/-}$ mice and wild-type littermates. Thus, CD19 functions in promoting BCR-mediated phosphoinositide hydrolysis via activation of PI3-kinase, and also supports antigen-induced phosphorylation of BCR receptor components and receptor activated kinases by an unknown mechanism. Since the src-family kinases Lyn and Lck are found associated with CD19 in unstimulated cells (5, 6), CD19 may mediate the latter effect via an increase in Ig-α phosphorylation by these kinases.

It has been demonstrated previously that wortmannin can inhibit angiotensin II–mediated IP_3 production in adrenal glomerulosa cells (48) as well as anti-DNP-IgE–mediated IP_3 production in RBL-2H3 cells (49). The mechanisms by which PI3-kinase affects inositol lipid hydrolysis is unclear. PLCγ1 and PLCγ2 are highly homologous enzymes; both contain two SH2 domains and one SH3 domain. In vitro studies suggest that tyrosine phosphorylation of the enzymes is required to increase the catalytic activity, but phosphatase treatment of phosphorylated PLCγ1 only partially inhibits PLCγ1-mediated inositol trisphosphate production (50), indicating that mechanisms other than tyrosine phosphorylation may regulate PLCγ1 activation. Our studies using the PI3-kinase inhibitor, wortmannin, indicate that antigen-stimulated inositol lipid turnover and calcium mobilization are dependent on PI3-kinase activation in B cells. Interestingly, induction of PLCγ1 and PLCγ2 tyrosine phosphorylation is relatively insensitive to wortmannin. As shown in Table II, IP_3 production is substantially inhibited by 10 nM wortmannin, while this concentration of wortmannin has a neglectable effect on PLCγ1 and PLCγ2 tyrosine phosphorylation. PI3-kinase phosphorylates the phosphoinositol containing lipids; PI, PI(4)P and $PI(4,5)P_2$ at the D3 position of the inositol ring (30). Two of the products of this phosphorylation, $PI(3,4)P_2$ and $PI(3,4,5)P_3$, are important regulators of cell proliferation (51). Recently it was suggested that $PI(3,4,5)P_3$ may play a role in signaling by associating with SH2 domains, and thereby modulating PI3-kinase association with tyrosine phosphorylated proteins (52). $PI(3,4,5)P_3$ could thereby regulate the activity of SH2 containing effector enzymes either directly or indirectly by relocating them. We suggest that this may reflect $PI(3,4,5)P_3$, the product of PI3-kinase, association with the SH2 domain of PLCγ1 and translocation of the enzyme to the plasma membrane where its substrate resides. Indeed addition of $PI(3,4,5)P_3$ to substrate vesicles has been shown to increase PLCγ hydrolysis of $PI(4,5)P_2$ (53). It has been demonstrated in other cell types that cell stimulation results in translocation of PLCγ1 and PLCγ2 from the cytosol to the membrane (54, 55). This suggests that activation of phosphatidylinositol hydrolysis involves both a PLCγ tyrosine phosphorylation event and a translocation event. Alternatively, or additionally, interactions between $PI(3,4,5)P_3$ and pleckstrin homology (PH) domains could be involved in translocation of effector proteins to the membrane to obtain optimal phosphoinositide hydrolysis and Ca^{2+} mobilization. A likely candidate is Bruton's tyrosine kinase, Btk, which has been shown to selectively interact with $PI(3,4,5)P_3$ vesicles via its PH domain (56). Indeed recent findings suggest that Btk is required for BCR-mediated Ca^{2+} mobilization; in particular for extracellular influx (Rawlings, D., personal communication). In this regard we do see a higher antigen-mediated inductive tyrosine phosphorylation of Btk in our CD19-positive plasmacytoma cell

line than in the CD19-negative line, suggesting that CD19 may influence the activation of Btk (results not shown). Recently it was shown in both T cells and B cells that under certain circumstances cell stimulation can lead to tyrosine phosphorylation of PLCγ, but no IP_3 production or calcium mobilization (41, 57–59). These examples further underscores the concept that tyrosine phosphorylation of PLCγ is not in itself sufficient to induce maximal IP_3 generation.

A critical role for CD19 phosphorylation in BCR activation of PI3-kinase, IP_3 production, and calcium mobilization is also supported by studies of FcγRIIB1 signal transduction. We and others have recently shown that coligation of BCR with FcγRIIB1 leads to rapid dephosphorylation of CD19 and failed PI3-kinase activation (60, 61). Therefore, FcγRIIB1-mediated CD19 dephosphorylation appears to prevent the normal contribution of CD19 to BCR signaling. Importantly, FcγRIIB1 cocrosslinking with BCR also results in aborted IP_3 production and reduced calcium mobilization. Thus, the calcium mobilization and IP_3 production phenotypes of the CD19-positive and -negative cell lines are clearly reminiscent of the signaling phenotypes of B cells stimulated with $F(ab')_2$ or intact antibodies, respectively (62, 63). $F(ab')_2$ stimulation leads to a strong increase in both intracellular and extracellular $[Ca^{2+}]_i$ mobilization, comparable to the antigen-mediated calcium mobilization in the CD19-positive cells, and a strong and sustained IP_3 production. In contrast coengagement of the FcγRIIB1 receptor by stimulation with intact antibodies only induces a transient production of IP_3, and calcium mobilization as seen in the CD19-negative B cell line (Figs. 2 and 3). These data support a role for CD19 and its effector PI3-kinase in BCR-mediated PLCγ activation and calcium mobilization.

Since our studies indicate that CD19 is required for maximal (i.e., both primary and secondary phase) Ca^{2+} mobilization, modulation of CD19 tyrosine phosphorylation, and resulting modulation of $[Ca^{2+}]_i$ mobilization pattern may be important in differentially regulating downstream signaling pathways such as activation of MAP kinase pathways, transcription factors, and proliferation/apoptosis responses (64, 65). Recently it was demonstrated that the amplitude and duration of Ca^{2+} signals contribute to transcriptional specificity (64). Such effects could at least in part be a consequence of the contribution of CD19, i.e., stimulation of B lymphocytes with $F(ab')_2$RAMIG, in which case CD19 is highly tyrosine phosphorylated, leads to a Ca^{2+} spike and a constant elevated second phase Ca^{2+} response. In contrast binding of immune complexes to FcγRIIB1 and the BCR, in which case CD19 tyrosine phosphorylation is decreased, results in a Ca^{2+} spike, but no prolonged second phase Ca^{2+} response triggering an effector output different from the $F(ab')_2$RAMIG stimulation. These modulations of the Ca^{2+} response may result in modulation of cell proliferation and apoptosis. Splenic B cells proliferate in response to B cell mitogens such as Staphylococcus aureus (SA) and anti-IgM. The SA-proliferation response is partially inhibited by the PI3-kinase inhibitor wortmannin (66), consistent with a role of PI3-kinase in BCR-mediated proliferation responses. CD19 activation may also be important for the regulation of apoptosis. When immune complexes are bound to the FcγRIIB1 and the BCR, in which case CD19 tyrosine phosphorylation is decreased, B cell proliferation is inhibited and cells undergo apoptosis (67). We hypothesize that this inhibition of proliferation and induction of apoptosis is a consequence of inhibition of PI3-kinase activity associated with CD19, leading to inhibition of downstream signaling pathways. Potentially FcγRIIB1-mediated inhibition of CD19 tyrosine phosphorylation and PI3-kinase activation could result in a failure to activate the serine/threonine protein kinase Akt/PKB, which has been shown to be a target of PI3-kinase (68–70), and is known to protect cells against apoptosis (71–73).

Here we have demonstrated a potential molecular basis for the essential role played by CD19 in antigen-mediated B cell activation, germinal center formation and generation of immune responses. CD19 functions as a constitutive component of the BCR signaling apparatus and is required for antigen-mediated BCR stimulation of PI3-kinase activation and, via PI3-kinase activation, phosphoinositide hydrolysis, and calcium mobilization. In fact, this is the first formal demonstration that CD19 modifies BCR signaling directly. The findings have important biological implications since CD19 and BCR expression are differentially regulated during B cell development. Variation of the ratio of expression of these molecules may provide a mechanism to vary the output of the receptor as a function of cell differentiation stage. Of potential importance in this context is the fact that the contribution of CD19 to BCR signaling is qualitative; it does not simply change the magnitude of the signal.

We thank Michael Reth for provision of the J558Lμm3 cells, Thomas Tedder for the hCD19 cDNA, and Marc Hertz for help with use of the JMP statistical analysis program, comments and reading of the manuscript.

A.M. Buhl is a Leukemia Society Research Fellow. J.C. Cambier is an Ida and Cecil Green Professor of Cell Biology. These studies were supported by the US Public Health Service.

Address correspondence to Dr. John C. Cambier, Division of Basic Sciences, Department of Pediatrics, National Jewish Research and Medical Center, 1400 Jackson St., Denver, CO 80206. Tel.: (303) 398-1325; FAX: (303) 398-1225; E-mail: cambierj@njc.org

Received for publication 10 July 1997 and in revised form 19 September 1997.

References

1. Fearon, D.T., and R.H. Carter. 1995. The CD19/CR2/TAPA-1 complex of B lymphocytes: linking natural to acquired immunity. *Ann. Rev. Immunol.* 13:127–149.
2. Carter, R.H., G.M. Doody, J.B. Bolen, and D.T. Fearon. 1997. Membrane IgM-induced tyrosine phosphorylation of CD19 requires a CD19 domain that mediates association with components of the B cell antigen receptor complex. *J. Immunol.* 158:3062–3069.
3. Tedder, T.F., and C.M. Isaacs. 1989. Isolation of cDNAs encoding the CD19 antigen of human and mouse B lymphocytes. A new member of the immunoglobulin superfamily. *J. Immunol.* 143:712–717.
4. Roifman, C.M., and S. Ke. 1993. CD19 is a substrate of the antigen receptor-associated protein tyrosine kinase in human B cells. *Biochem. Biophys. Res. Commun.* 194:222–225.
5. Uckun, F.M., A.L. Burkhardt, L. Jarvis, X. Jun, B. Stealey, I. Dibirdik, D.E. Myers, A.L. Tuel, and J.B. Bolen. 1993. Signal transduction through the CD19 receptor during discrete developmental stages of human B-cell ontogeny. *J. Biol. Chem.* 268:21172–21184.
6. van Noesel, C.J.M., A.C. Lankester, G.M.W. van Schijndel, and R.A.W. van Lier. 1993. The CR2/CD19 complex on human B cells contains the src-family kinase Lyn. *Intl. Immunol.* 5:699–705.
7. Tedder, T.F., L.J. Zhou, and P. Engel. 1994. The CD19/CD21 signal transduction complex of B lymphocytes. *Immunol. Today* 15:437–442.
8. Chalupny, N.J., A. Aruffo, J.M. Esselstyn, P.-Y. Chan, J. Bajorath, J. Blake, L.K. Gilliland, J.A. Ledbetter, and M.A. Tepper. 1995. Specific binding of Fyn and phosphatidylinositol 3-kinase to the B cell surface glycoprotein CD19 through their src homology 2 domains. *Eur. J. Immunol.* 25:2978–2984.
9. Tuveson, D.A., R.H. Carter, S.P. Soltoff, and D.T. Fearon. 1993. CD19 of B cells as a surrogate kinase insert region to bind phosphatidylinositol 3-kinase. *Science.* 260:986–989.
10. Weng, W.-K., L. Jarvis, and T.W. LeBien. 1994. Signaling through CD19 activates Vav/mitogen-activated protein kinase pathway and induces formation of a CD19/Vav/phosphatidylinositol 3-kinase complex in human B cell precursors. *J. Biol. Chem.* 269:32514–32521.
11. Songyang, Z., S.E. Shoelson, J. McGlade, P. Olivier, T. Pawson, X.R. Bustelo, M. Barbacid, H. Sabe, H. Hanafusa, T. Yi et al. 1994. Specific motifs recognized by the SH2 domains of Csk, 3BP2, fps/fes, GRB-2, HCP, SHC, Syk, and Vav. *Mol. Cell. Biol.* 14:2777–2785.
12. Gilliland, L.K., G.L. Schieven, N.A. Norris, S.B. Kanner, A. Aruffo, and J.A. Ledbetter. 1992. Lymphocyte lineage-restricted tyrosine-phosphorylated proteins that bind PLC gamma 1 SH2 domains. *J. Biol. Chem.* 267, no. 19:13610–13616.
13. Chalupny, N.J., S.B. Kanner, G.L. Schieven, S. Wee, L.K. Gilliland, A. Aruffo, and J.A. Ledbetter. 1993. Tyrosine phosphorylation of CD19 in pre-B and mature B cells. *EMBO (Eur. Mol. Biol. Organ.) J.* 12:2691–2696.
14. Matsumoto, A.K., B.J. Kopicky, R.H. Carter, D.A. Tuveson, T.F. Tedder, and D.T. Fearon. 1991. Intersection of the complement and immune systems: a signal transduction complex of the B lymphocyte-containing complement receptor type 2 and CD19. *J. Exp. Med.* 173:55–64.
15. Bradbury, L.E., G.S. Kansas, S. Levy, R.L. Evans, and T.F. Tedder. 1992. The CD19/CD21 signal transducing complex of human B lymphocytes includes the target of antiproliferative antibody-1 and Leu-13 molecules. *J. Immunol.* 149:2841–2850.
16. Matsumoto, A.K., D.R. Martin, R.H. Carter, L.B. Klickstein, J.M. Ahearn, and D.T. Fearon. 1993. Functional dissection of the CD21/CD19/TAPA-1/Leu-13 complex of B lymphocytes. *J. Exp. Med.* 178,:1407–1417.
17. Lankester, A.C., G.M.W. van Schijndel, P.M.L. Rood, A.J. Verhoeven, and R.A.W. van Lier. 1994. B cell antigen receptor cross-linking induces tyrosine phosphorylation and membrane translocation of a multimeric Shc complex that is augmented by CD19 co-ligation. *Eur. J. Immunol.* 24:2818–2825.
18. Lankester, A.C., P.M.L. Rood, G.M.W. van Schijudel, B. Hoodbrink, A.J. Verhoeven, and R.A.W. van Lier. 1996. Alteration of B-cell antigen receptor signaling by CD19 co-ligation. A study with bispecific antibodies. *J. Biol. Chem.* 271: 22326–22330.
19. Carter, R.H., D.A. Tuveson, D.J. Park, S.G. Rhee, and D.T. Fearon. 1991. The CD19 complex of B lymphocytes. Activation of phospholipase C by a protein tyrosine kinase-dependent pathway that can be enhanced by the membrane IgM complex. *J. Immunol.* 147:3663–3671.
20. Carter, R.H., and D.T. Fearon. 1992. CD19: lowering the threshold for antigen receptor stimulation of B lymphocytes. *Science.* 256:105–107.
21. Dempsey, P.W., M.E. Allison, S. Akkaraju, C.C. Goodnow, and D.T. Fearon. 1996. C3d of complement as a molecular adjuvant: bridging innate and acquired immunity. *Science.* 271: 348–350.
22. Krop, I., A.L. Shaffer, D.T. Fearon, and M.S. Schlissel. 1996. The signaling activity of murine CD19 is regulated during B cell development. *J. Immunol.* 157:48–56.
23. Ledbetter, J.A., P.S. Rabinovitch, C.H. June, C.W. Song, E.A. Clark, and F.M. Uckun. 1988. Antigen-independent regulation of cytoplasmic calcium in B cells with a 12-kD B-cell growth factor and anti-CD19. *Proc. Natl. Acad. Sci. USA.* 85: 1897–1901.
24. Pesando, J.M., L.S. Bouchard, and B.E. McMaster. 1989. CD19 is functionally and physically associated with surface immunoglobulin. *J. Exp. Med.* 170:2159–2163.
25. Rijkers, G.T., A.W. Griffioen, B.J. Zegers, and J.C. Cambier. 1990. Ligation of membrane immunoglobulin leads to inactivation of the signal-transducing ability of membrane immunoglobulin, CD19, CD21, and B-cell gp95. *Proc. Natl. Acad. Sci. USA.* 87:8766–8770.
26. Engel, P., L.-J. Zhou, D.C. Ord, S. Sato, B. Koller, and T.F. Tedder. 1995. Abnormal B lymphocyte development, activation, and differentiation in mice that lack or overexpress the CD19 signal transduction molecule. *Immunity.* 3:39–50.
27. Rickert, R.C., K. Rajewsky, and J. Roes. 1995. Impairment of T-cell-dependent B-cell responses and B-1 cell development in CD19-deficient mice. *Nature.* 376:352–355.
28. Justement, L.B., K.S. Campbell, N.C. Chien, and J.C. Cambier. 1991. Regulation of B cell antigen receptor signal transduction and phosphorylation by CD45. *Science.* 252:1839–1842.
29. Couture, C., G. Baier, C. Oetken, S. Williams, D. Telford, A. Marie-Cardine, G. Baier-Bitterlich, S. Fischer, P. Burn, A. Altman, and T. Mustelin. 1994. Activation of $p56^{lck}$ by $p72^{syk}$ through physical association and N-terminal tyrosine phosphorylation. *Mol. Cell. Biol.* 14:5249–5258.
30. Whitman, M., C.P. Downes, M. Keeler, T. Keller, and L.

Cantley. 1988. Type I phosphatidylinositol kinase makes a novel inositol phospholipid, phosphatidylinositol-3-phosphate. *Nature*. 332:644–646.
31. Campbell, K.S., E.J. Hager, R.J. Friedrich, and J.C. Cambier. 1991. IgM antigen receptor complex contains phosphoprotein products of B29 and mb-1 genes. *Proc. Natl. Acad. Sci. USA*. 88:3982–3986.
32. Hombach, J., L. Leclercq, A. Radbruch, K. Rajewsky, and M. Reth. 1988. A novel 34-kd protein co-isolated with the IgM molecule in surface IgM-expressing cells. *EMBO (Eur. Mol. Biol. Organ.) J.* 7:3451–3456.
33. Zhou, L.-J., D.C. Ord, S.A. Omori, and T.F. Tedder. 1992. Structure of the genes encoding the CD19 antigen of human and mouse B lymphocytes. *Immunogenetics*. 35:102–111.
34. Sato, S., D.A. Steeber, P.J. Jansen, and T.F. Tedder. 1997. CD19 expression levels regulate B lymphocyte development. *J. Immunol*. 158:4662–4669.
35. Krop, I., A.R. de Fougerolles, R.R. Hardy, M. Allison, M.S. Schlissel, and D.T. Fearon. 1996. Self-renewal of B-1 lymphocytes is dependent on CD19. *Eur. J. Immunol.* 26:238–242.
36. Putney, J.J. 1993. Excitement about calcium signaling in inexcitable cells. *Science*. 262:676–678.
37. Clark, M.R., K.S. Campbell, A. Kazlauskas, S.A. Johnson, M. Hertz, T.A. Potter, C. Pleiman, and J.C. Cambier. 1992. The B cell antigen receptor complex: association of Ig-alpha and Ig-beta with distinct cytoplasmic effectors. *Science*. 258: 123–126.
38. Law, D.A., V.W.F. Chan, S.K. Datta, and A.L. DeFranco. 1993. B-cell antigen receptor motifs have redundant signaling capabilities and bind the tyrosine kinases PTK72, Lyn and Fyn. *Curr. Biol*. 3:645–657.
39. Johnson, S.A., C.M. Pleiman, L. Pao, J. Schneringer, K. Hippen, and J.C. Cambier. 1995. Phosphorylated immunoreceptor signaling motifs (ITAMs) exhibit unique abilities to bind and activate Lyn and syk tyrosine kinases. *J. Immunol*. 155: 4596–4603.
40. Cambier, J.C. 1995. Antigen and Fc receptor signaling. *J. Immunol*. 155:3281–3285.
41. Pao, L.I., W.D. Bedzyk, C. Persin, and J.C. Cambier. 1997. Molecular targets of CD45 in B cell antigen receptor signal transduction. *J. Immunol*. 158:1116–1124.
42. Pleiman, C.M., W.M. Hertz, and J.C. Cambier. 1994. Activation of phosphatidylinositol-3′ kinase by Src-family kinase SH3 binding to the p85 subunit. *Science*. 263:1609–1612.
43. Wymann, M.P., G. Bulgarelli-Leva, M.J. Zvelebil, L. Pirola, B. Vanhaesebroeck, M.D. Waterfield, and G. Panayotou. 1996. Wortmannin inactivates phosphoinositide 3-kinase by covalent modification of Lys-802, a residue involved in the phosphate transfer reaction. *Mol. Cell. Biol*. 16:1722–1733.
44. Vlahos, C.J., W.F. Matter, K.Y. Hui, and R.F. Brown. 1994. A specific inhibitor of phosphatidylinositol 3-kinase, 2-(4-morpholinyl)-8-phenyl-4H-1-benzopyran-4-one (LY294002). *J. Biol. Chem*. 269:5241–5248.
45. Zhou, L.J., H.M. Smith, T.J. Waldschmidt, R. Schwating, J. Daley, and T.F. Tedder. 1994. Tissue-specific expression of the human CD19 gene in transgenic mice inhibits antigen-independent B-lymphocyte development. *Mol. Cell. Biol.* 14: 3884–3894.
46. Sato, S., N. Ono, D.A. Steeber, D.S. Pisetsky, and T.F. Tedder. 1996. CD19 regulates b lymphocyte signaling thresholds critical for the development of B-1 lineage cells and autoimmunity. *J. Immunol*. 157:4371–4378.
47. Sato, S., D.A. Steeber, and T.F. Tedder. 1995. The CD19 signal transduction molecule is a response regulator of B-lymphocyte differentiation. *Proc. Natl. Acad. Sci. USA*. 92: 11558–11562.
48. Nakanishi, S., K.J. Catt, and T. Balla. 1994. Inhibition of agonist-stimulated inositol 1,4,5-trisphosphate production and calcium signaling by the myosin light chain kinase inhibitor, wortmannin. *J. Biol. Chem.* 269:6528–6535.
49. Barker, S.A., K.K. Caldwell, A. Hall, A.M. Martinez, J.R. Pfeiffer, J.M. Oliver, and B.S. Wilson. 1995. Wortmannin blocks lipid and protein kinase activities associated with PI 3-kinase and inhibits a subset of responses induced by Fc epsilon R1 cross-linking. *Mol. Biol. Cell*. 6:1145–1158.
50. Nishibe, S., M.I. Wahl, S.M.T. Hernandez-Sotomayor, N.K. Tonks, S.G. Rhee, and G. Carpenter. 1990. Increase of the catalytic activity of phospholipase C-γ1 by tyrosine phosphorylation. *Science*. 250:1253–1256.
51. Cantley, L.C., K.R. Auger, C. Carpenter, B. Duckworth, A. Graziani, R. Kapeller, and S. Soltoff. 1991. Oncogenes and signal transduction. *Cell*. 64:281–302 (erratum published 65:915).
52. Rameh, L.E., C.S. Chen, and L.C. Cantley. 1995. Phosphatidylinositol (3,4,5)P_3 interacts with SH2 domains and modulates PI 3-kinase association with tyrosine-phosphorylated proteins. *Cell*. 83:821–830.
53. Rhee, S.G., and Y.S. Bae. 1997. Regulation of phosphoinositide-specific phospholipase C isozymes. *J. Biol. Chem*. 272: 15045–15048
54. Atkinson, T.P., M.A. Kaliner, and R.J. Hohman. 1992. Phospholipase C-γ1 is translocated to the membrane of rat basophilic leukemia cells in response to aggregation of IgE receptors. *J. Immunol*. 148:2194–2200.
55. Atkinson, T.P., C.W. Lee, S.G. Rhee, and R.J. Hohman. 1993. Orthovanadate induces translocation of phospholipase C-gamma 1 and -gamma 2 in permeabilized mast cells. *J. Immunol*. 151:1448–1455.
56. Salim, K., M.J. Bottomley, E. Querfurth, M.J. Zvelebil, I. Gout, R. Scaife, R.L. Margolis, R. Gigg, C.I.E. Smith, P.C. Driscoll et al. 1996. Distinct specificity in the recognition of phosphoinositides by the pleckstrin homology domains of dynamin and Bruton's tyrosine kinase. *EMBO (Eur. Mol. Biol. Organ.) J.* 15:6241–6250.
57. Rigley, K., P. Slocombe, K. Proudfoot, S. Wahid, K. Mandair, and C. Bebbington. 1995. Human p59fyn(T) regulates OKT3-induced calcium influx by a mechanism distinct from PIP2 hydrolysis in Jurkat T cells. *J. Immunol.* 154:1136–1145 (erratum published 154:4223).
58. Motto, D.G., M.A. Musci, S.E. Ross, and G.A. Koretsky. 1996. Tyrosine phosphorylation of Grb2-associated proteins correlates with phospholipase Cγ1 activation in T cells. *Mol. Cell. Biol*. 16:2823–2829.
59. Jensen, W.A., C.M. Pleiman, P. Beaufils, A.-M. Wegener, B. Malissen, and J.C. Cambier. 1997. Qualitatively distinct signaling through T cell antigen receptor subunits. *Eur. J. Immunol*. 27:707–716.
60. Kiener, P.A., M.N. Lioubin, L.R. Rohrschneider, J.A. Ledbetter, S.G. Nadler, and M.L. Diegel. 1997. Co-ligation of the antigen and Fc receptors gives rise to the selective modulation of intracellular signaling in B cells. *J. Biol. Chem*. 272: 3838–3844.
61. Hippen, K.L., A.M. Buhl, D. D'Ambrosio, K. Nakamura, C. Persin, and J.C. Cambier. 1997. FcγRIIB1 inhibition of BCR mediated phosphoinositide hydrolysis and Ca^{2+} mobilization is integrated by CD19 dephosphorylation. *Immunity*. 7:49–58.
62. Bijsterbosch, M.K., and G.G. Klaus. 1985. Crosslinking of

surface immunoglobulin and Fc receptors on B lymphocytes inhibits stimulation of inositol phospholipid breakdown via the antigen receptors. *J. Exp. Med.* 162:1825–1836.

63. Wilson, H.A., D. Greenblatt, C.W. Taylor, J.W. Putney, R.Y. Tsien, F.D. Finkelman, and T.M. Chused. 1987. The B lymphocyte calcium response to anti-Ig is diminished by membrane immunoglobulin cross-linkage to the Fc gamma receptor. *J. Immunol.* 138:1712–1718.
64. Dolmetsch, R.E., R.S. Lewis, C.C. Goodnow, and J.I. Healy. 1997. Differential activation of transcription factors induced by Ca^{2+} response amplitude and duration. *Nature*. 386:855–858.
65. Healy, J.I., R.E. Dolmetsch, L.A. Timmermann, J.G. Cyster, M.L. Thomas, G.R. Crabtree, R.S. Lewis, and C.C. Goodnow. 1997. Different nuclear signals are activated by the B cell receptor during positive versus negative signaling. *Immunity*. 6:419–428.
66. Aagaard-Tillery, K.M., and D.F. Jelinek. 1996. Phosphatidylinositol 3-kinase activation in normal human B lymphocytes. *J. Immunol.* 156:4543–4554.
67. Ashman, R.F., D. Peckham, and L.L. Stunz. 1996. Fc receptor off-signal in the B cell involves apoptosis. *J. Immunol.* 157: 5–11.
68. Burgering, B.M.T., and P.J. Coffer. 1995. Protein kinase B (c-Akt) in phosphatidylinositol-3-OH kinase signal transduction. *Nature*. 376:599–602.
69. Datta, K., A. Bellacosa, T.O. Chan, and P.N. Tsichlis. 1996. Akt is a direct target of the phosphatidylinositol 3-kinase. *J. Biol. Chem.* 271:30835–30839.
70. Franke, T.F., D.R. Kaplan, L.C. Cantley, and A. Toker. 1997. Direct regulation of the Akt proto-oncogene product by phosphatidylinositol-3,4-bisphosphate. *Science.* 275:665–668.
71. Dudek, H., S.R. Datta, T.F. Franke, M.J. Birnbaum, R. Yao, G.M. Cooper, R.A. Segal, D.R. Kaplan, and M.E. Greenberg. 1997. Regulation of neuronal survival by the serine-threonine protein kinase Akt. *Science*. 275:661–665.
72. Kauffmann-Zeh, A., P. Rodriguez-Viciana, E. Ulrich, C. Gilbert, P. Coffer, J. Downward, and G. Evan. 1997. Suppression of c-Myc-induced apoptosis by Ras signaling through PI(3)K and PKB. *Nature*. 385:544–548.
73. Kulik, G., A. Klippel, and M.J. Weber. 1997. Antiapoptotic signaling by the insulin-like growth factor I receptor, phosphatidylinositol 3-kinase, and Akt. *Mol. Cell. Biol*. 17:1595–1606.
74. CalCalc—A Program to Calculate Calcium Concentrations in the Presence of EGTA Department of Biochemistry, Colorado State University, Fort Collins, Colorado.
75. Grynkiewicz, G., M. Poenie, and R.Y. Tsien. 1985. A new generation of Ca^{2+} indicators with greatly improved fluorescence properties. *J. Biol. Chem*. 260:3440–3450.